PAPER

Ligand assisted carbon dioxide activation and hydrogenation using molybdenum and tungsten amides†

Subrata Chakraborty, Olivier Blacque and Heinz Berke*

The hepta-coordinated isomeric $M(NO)Cl_3(PN^HP)$ complexes {M = Mo, **1a(syn,anti)**; W, **1b(syn,anti)**, $PN^HP = (iPr_2PCH_2CH_2)_2NH$, ($H_N$ atom of PN^HP syn and anti to the NO ligand)} and the paramagnetic species $M(NO)Cl_2(PN^HP)$ (M = Mo, **2a(syn,anti)**; W, **2b(syn,anti)**) could be prepared via a new synthetic pathway. The pseudo trigonal bipyramidal amides M(NO)(CO)(PNP) {M = Mo, **3a**; W, **3b**; $[PNP]^-$ = $[(iPr_2PCH_2CH_2)_2N]^-$} were reacted with CO_2 at room temperature with CO_2 approaching the M≡N double bond in the equatorial (CO,NO,N) plane trans to the NO ligand and forming the pseudo-octahedral cyclic carbamates M(NO)(CO)(PNP)(OCO) (M = Mo, **4a(trans)**; W = **4b(trans)**). DFT calculations revealed that the approach to form the **4b(trans)** isomer is kinetically determined. The amine hydrides M(NO)H(CO)-(PN^HP) {M = Mo, **5a(cis,trans)**; W, **5b(cis,trans)**}, obtained by H_2 addition to **3a,b**, insert CO_2 (2 bar) at room temperature into the M–H bond generating isomeric mixtures of the η^1-formato complexes $M(NO)(CO)(PN^HP)(\eta^1\text{-OCHO})$, (M = Mo, **6a(cis,trans)**; M = W, **6b(cis,trans)**). Closing the stoichiometric cycles for sodium formate formation the **6a,b(cis,trans)** isomeric mixtures were reacted with 1 equiv. of $Na[N(SiMe_3)_2]$ regenerating **3a,b**. Attempts to turn the stoichiometric formate production into catalytic CO_2 hydrogenation using **3a,b** in the presence of various types of sterically congested bases furnished yields of formate salts of up to 4%.

Introduction

Carbon dioxide is one of the main carbon sources and although it is abundant and inexpensive, its utilization as feedstock for commodity chemicals is insufficiently explored.[1] CO_2 being a thermodynamically and kinetically stable molecule a promising approach to overcome its often too low reactivity would be its metal mediated "activation".[2,3a] In fact recent years have seen tremendous efforts to activate and reduce CO_2 and to employ it as a C_1 building block for chemical synthesis.[3] Activation by binding to a metal center and subsequent reaction modes of the CO_2 depend on the type of the CO_2 binding. There are three possible ways of CO_2 coordination as depicted in Fig. 1.[1b]

Lately metal ligand cooperation (MLC) has been explored as a way to activate H_2 or small molecules with C–H, N–H, O–H moieties.[4,5] MLC would be a promising approach for CO_2 activation, but reported examples of such CO_2 activation are

Departent of Chemistry, University of Zürich, Winterthurerstrasse 190, 8057 Zürich, Switzerland. E-mail: hberke@chem.uzh.ch
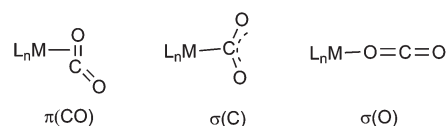
Fig. 1 Possible binding modes of CO_2 to a metal centre.

M = Ru, L = H; P = PtBu₂
M = Re; L = CO; P = PtBu₂

M = Mo, W; P = PiPr₂
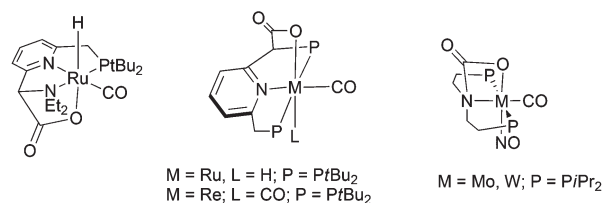
Fig. 2 Metal–ligand cooperation in CO_2 activation.

scarce. Only recently Sanford and coworkers have demonstrated that (PNN)Ru(H)(CO) pincer systems take up CO_2 at room temperature involving C–C bond formation between the unsaturated arm of the pincer ligand and the electrophilic carbon atom of CO_2 (Fig. 2).[6] Milstein and coworkers investi-

gated related types of reversible CO_2 binding employing unsaturated PNP pincer complexes of Ru and Re (Fig. 2).[7]

"Metal-free" CO_2 activation was accomplished using Frustrated Lewis Pair (FLP) type chemistry.[8] In this context it seems also worth mentioning that a transition metal based $L_nRe\text{-}H/B(C_6F_5)_3$ systems can activate CO_2 in a FLP type manner, where the metal hydride species took the role of the FLP Lewis base component.[9] Activation of CO_2 is anticipated to be preceding its hydrogenation, which may then lead to formic acid, but also can continue in the reduction sequence forming products with higher hydrogen contents, which like formic acid could in principle function as reversible H_2 storage materials.[10] Though the reaction of H_2 with CO_2 to obtain formic acid is exothermic ($\Delta H = -8$ kcal mol^{-1}), it is endergonic with $\Delta G = 8$ kcal mol^{-1} due to gaseous starting materials. Therefore an additional thermodynamic driving force has to be provided, like for instance pressure and the addition of a base inducing salt formation or stabilizing acid–base hydrogen bonding interactions[3] causing a shift of the equilibrium towards the formic acid side.

Advances in the efficiency of homogeneous hydrogenation catalysis of CO_2 were recently reported with late transition metal complexes,[11,12] but somewhat different from these developments it is one of the aims of this research to replace the platinum group metals ruthenium,[13–15] rhodium[16,17] and iridium[18,19] with non-precious metals.[20] In this regard molybdenum and tungsten based reductions of CO_2 are challenging objectives. Despite some recent achievements in molybdenum and tungsten catalysed homogeneous hydrogenations[21] and related hydrosilylations,[22] and our group's recent accomplishments in bifunctional imine hydrogenations,[23a] the stepwise ionic hydrogenation of imines,[23b,c] Osborn type olefin hydrogenations[24] and nitrile hydrogenations,[25] the homogeneous hydrogenation of carbon dioxide could not be achieved with compounds of these metals till date.

In this paper a carbon dioxide activation mode supported by MLC could be established as shown in Fig. 2. Furthermore, stoichiometric hydrogenation of CO_2 turned out to be accessible using the previously reported molybdenum and tungsten amides **3a,b**.[23a]

Results and discussion

Preparation of M(II) and M(I) (M = Mo, W) complexes bearing (iPr$_2$PCH$_2$CH$_2$)$_2$NH ligand

Reaction of (iPr$_2$PCH$_2$CH$_2$)$_2$NH (PN^{H}P) ligand with the M(NO)-Cl$_3$(NCMe)$_2$ complexes (M = Mo, W) led at room temperature in THF to precipitation of the isomeric mixtures of Mo(NO)-Cl$_3$(PN^{H}P), **1a(syn,anti)** and W(NO)Cl$_3$(PN^{H}P), **1b(syn,anti)**) in moderate yields (**1a(syn,anti)**, 55%; **1b(syn,anti)**, 62%) (Scheme 1).

The *syn* and *anti* notation for the isomers of **1a,b(syn,anti)** correspond to the relative position of the H$_N$ atom at the internal N atom of the PN^{H}P ligand with respect to the NO ligand. The spectroscopic yields of *syn* and *anti* isomers of
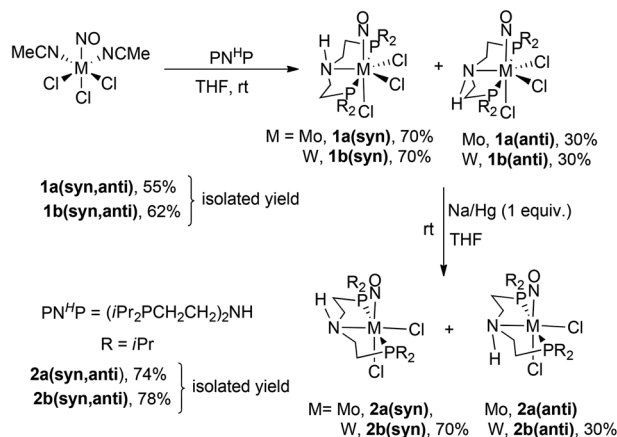
Scheme 1 Preparation of the isomeric mixture of M(II)(NO)Cl$_3$(PN^{H}P), **1a,b(syn,anti)**) and reduction to M(I)(NO)Cl$_2$(PN^{H}P), **2a,b(syn,anti)** complexes (M = Mo,W).

both **1a,b(syn,anti)** are given in Scheme 1. The isomers of **1a-(syn,anti)** and **1b(syn,anti)** were found to be reasonably soluble only in CH_2Cl_2. The $^{31}P\{^1H\}$ NMR spectra of the isomeric mixture of **1a(syn,anti)** revealed two singlets at δ 69.3 ppm (**1a-(syn)**) and 71 ppm (**1a(anti)**) in a ratio of 7 : 3 indicating equivalence of both phosphorus atoms of each isomer of **1a(syn, anti)** (Fig. 3, left). The $^{31}P\{^1H\}$ NMR spectra of the isomeric mixture of **1b(syn,anti)** exhibited also two singlets, but in this case along with tungsten satellites at δ 56.8 ppm (s, $^1J_{P–W}$ (d, satellite) = 184.8 Hz, **1b(syn)**)) and 58.3 (s, $^1J_{P–W}$ (d, satellite) = 189.3 Hz, **1b(anti)**)) assigned to the equivalent phosphorus atoms of each *syn* and *anti* isomer (Fig. 3, right).

In the IR spectra of **1a,b(syn,anti)** the isomers could not be distinguished, which showed only one sharp band for the molybdenum and tungsten complexes at 1653 and 1596 cm^{-1}, respectively, attributed to the ν_{NO} vibrations. The ^1H NMR spectra of the isomeric mixtures of **1a,b(syn,anti)** exhibited several doubled signals for the methyl, methyne and methylene protons appearing in the expected region with strong overlap of the signals of the *syn* and *anti* isomers impeding their distinct assignment. In the ^1H NMR spectra a conspicuous signal appeared at δ 4.4 ppm, which was assigned to the H$_N$ atom of **1a(syn)**. However, the H$_N$ atom of **1a(anti)** could not be assigned in the ^1H NMR spectrum presumably owing to the quite low concentration of this isomer and overlap of the signal with the signal of the CH_2Cl_2 solvent. The H$_N$ atoms of the isomeric mixture of **1b(syn,anti)** appeared as broad singlets at δ 4.47 ppm and 5.50 ppm in the ^1H NMR spectra and based on the different intensity these could be assigned to the **1b(syn)** and **1b(anti)** isomers, respectively. The virtual triplet signal in the $^{13}C\{^1H\}$ NMR at δ 55.9 (t, $^vJ_{C–P}$ = 3.6 Hz) ppm for isomeric mixture of **1a(syn,anti)** was attributed to the carbon atoms of **1a(syn)** isomer adjacent to the nitrogen atom of the PN^{H}P ligand and the related signals of **1b(anti)** could not be detected. On the other hand the virtual $^{13}C\{^1H\}$ NMR triplets at δ 55.9 (t, $^vJ_{C–P}$ = 5.9 Hz) ppm for **1b(syn)** and at 55 ppm
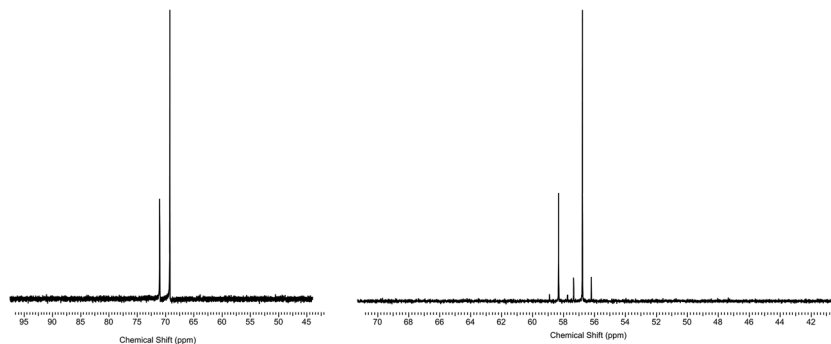
Fig. 3 $^{31}P\{^1H\}$ NMR spectra of the isomeric mixture of Mo(NO)Cl$_3$(PN^{H}P), **1a(*syn,anti*)** {left, **1a(*syn*)**, 70%; **1a(*anti*)**, 30%} and the isomeric mixture of W(NO)Cl$_3$(PN^{H}P), **1b(*syn,anti*)** {right, **1b(*syn*)**, 70%; **1b(*anti*)**, 30%} at room temperature in CD$_2$Cl$_2$.

(t, $^vJ_{C-P}$ 4.8 Hz) for **1b(*anti*)** could be assigned to the N-adjacent carbon atoms. Several attempts failed to grow suitable single crystals for X-ray diffraction studies of any isomer of the **1a,b-(*syn,anti*)** mixture, but **1a,b(*syn,anti*)** could be fully characterized by ^1H NMR, $^{31}P\{^1H\}$ NMR, $^{13}C\{^1H\}$ NMR, IR and mass spectrometry, and the compositions were established by elemental analyses.

1a,b(*syn,anti*) are heptacoordinated diamagnetic species with the metal centers in +II oxidation states. Our initial attempts to deprotonate the N–H moiety of **1a(*syn,anti*)** applying NaN(SiMe$_3$)$_2$ to obtain 16 e$^-$ unsaturated amido complex[23a] failed, which led to inseparable mixtures of products and could not be identified. Attempts to reduce **1a,b(*syn,anti*)** by 1-electron reducing agents led to paramagnetic M(+I) species (M = Mo, W). Further reduction to M(0) species seemed difficult with the given strongly electron donating coordinative environment.

The reaction of **1a,b(*syn,anti*)** with approximately one equivalent of 1% Na/Hg in THF at room temperature resulted in the formation of green isomeric mixtures of Mo(I)(NO)Cl$_2$(PN^{H}P) complexes (**2a(*syn,anti*)**) or of W(I)(NO)Cl$_2$(PN^{H}P) (**2b(*syn,anti*)**) in 74% and 78% yields, respectively (Scheme 1). **2a,b(*syn,anti*)** were found quite soluble in THF and CH$_2$Cl$_2$, but were sparingly soluble in toluene and benzene. In the $^{31}P\{^1H\}$ and ^1H NMR spectra of the isomeric mixtures of **2a,b(*syn,anti*)** no signals could be observed due to the paramagnetic nature of these complexes. The inaccessibility of ^1H and $^{31}P\{^1H\}$ NMR spectra impeded estimates of spectroscopic yields of the *syn* and *anti* isomers in solution. Thus, the isomeric mixtures of **2a,b(*syn,anti*)** were characterized by IR and EPR spectroscopy, elemental analyses and X-ray diffraction studies. Sharp bands at 1595 and 1547 cm^{-1} for the isomeric mixtures of **2a,b(*syn,anti*)** were assigned to ν_{NO} vibrations, respectively, which appeared at lower wave numbers than those of **1a,b(*syn, anti*)** indicating a higher degree of back-donation from the metal center to the nitrosyl ligand. Single crystals suitable for X-ray diffraction studies were grown from the isomeric mixtures of **2a,b(*syn,anti*)** from concentrated toluene–pentane mixtures at −30 °C. The crystal structure determination revealed preferential crystallization of the **2a(*anti*)** and **2b(*syn*)**

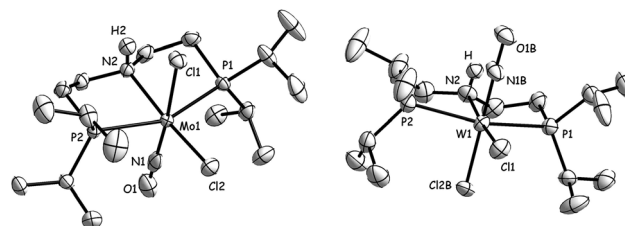**Fig. 4** Molecular structures of M(NO)Cl$_2$(PN^{H}P), {M = Mo; **2a(*anti*)** (left); W, **2b(*syn*)** (right)} Thermal ellipsoids are drawn at the 50% probability level. Selected bond distances (Å) and bond angles (°) for **2a(*anti*)**: Mo1−N2 2.255(2), Mo1−N1 1.855(3), Mo1−Cl1 2.5021(7), Mo1−P1 2.5372(7), N2−H2 0.91, P2−Mo1−P 1156.25(2), P2−Mo1−Cl2 100.64(2), P2−Mo1−Cl1 87.04(2), Mo1−N1−O1 178.7(3). Selected bond distances(Å) and bond angles (°) for **2b(*syn*)**: W1−N2 2.232(4), W1−N1B 1.811(19), W1−P1 2.5123(13), W1−Cl2B 2.381(6), N2−H 0.79 (4), P2−W1−P1 157.23(4), P2−W1−N2 78.82(13), W1−N1B−O1B 178(3), N1B−W1−Cl2B 172.2(8).

isomers. Both of them crystallized in the orthorhombic space group $P2_12_12_1$. The molecular structures revealed neutral pseudo-octahedral complexes. Perspective views with selected bond distances and bond angles of **2a(*anti*)** and **2b(*syn*)** are shown in Fig. 4. The two phosphorus atoms and the nitrogen atom of the PN^{H}P ligand and the two chloride ligands attached to the metal center occupy "equatorial" positions in both cases. The H$_N$ proton and the nitrosyl ligand were found to be disposed *anti* indicating the presence of the *anti* **2a(*anti*)** isomer. No NO/Cl disorder was found in the structure of **2a(*anti*)**, but despite this, the presence of isomeric mixtures in solution with one prevailing component could not fully be ruled out.

On the other hand the crystal structure analysis of **2b(*syn*)** revealed that the structure had *trans* NO/Cl disorder over two positions with site occupancy factors of 0.698(8) and 0.302(8). This NO/Cl disorder again supports the presence of the isomeric mixtures with respect to the H$_N$ position and the nitrosyl ligand and the presence of the *syn* and *anti* isomer in an approximately 7 : 3 ratio in the solid state. An inversion at the N atom with prototropic rearrangement at this atom seemed at least not to occur in the solid state. This would be also in

accord with the assignment of the same *syn/anti* ratio for the precursors **1a,b(syn,anti)**. The isomeric mixtures of **2a,b-(syn,anti)** are rare paramagnetic complexes with the metal centers in +I oxidation state and of low-spin d^5 configurations. To probe the paramagnetic nature, solution EPR measurements were carried out on **2a,b(syn,anti)** in toluene at room temperature. The spectra are displayed in the ESI section (Fig. S1†).

We then attempted deprotonation of the H_N proton of the PN^{H}P ligand backbone of **2a,b(syn,anti)** employing Na[N(SiMe$_3$)$_2$], which led to decomposition and the solution turned black immediately. Moreover, attempts were also undertaken to prepare the previously reported M(NO)(CO)(PNP) {M = Mo, **3a**; W, **3b**} amides[23a] *via* a new synthetic route starting from the **2a,b(syn,anti)**.

Reduction of **2a,b(syn,anti)** in the presence of 1 bar CO and 1% Na/Hg at room temperature showed the formation of several unidentified species instead of the expected unique complex of an isomeric carbonyl chloride M(NO)(CO)Cl(PN^{H}P) (M = Mo, W), which prevented concomitant deprotonation to obtain the requested M(NO)(CO)(PNP) (M = Mo, **3a**; W, **3b**).

Nevertheless M(NO)(CO)(PNP) **3a,b** could be prepared according to our previously published procedure[23a] starting from M(NO)(CO)$_4$(ClAlCl$_3$) and PN^{H}P ligand followed by deprotonation with NaN(SiMe$_3$)$_2$ and tested their reactivity with CO$_2$ and their hydrogenation capability.

## Reactivity of the M(NO)(CO)(PNP) {M = Mo, 3a W, 3b} amide complexes with CO$_2$

Reaction of M(NO)(CO)(PNP) {M = Mo, **3a** W, **3b**; PNP = N(CH$_2$CH$_2$PiPr$_2$)$_2$} with CO$_2$ (2 bar) at room temperature in THF led to formation of the 2 + 2 addition products across the M=N bonds, the carbamate complexes Mo,W(NO)(CO)(PNP)(OCO) **4a,b(trans)** (Scheme 2). The specification "*trans*" refers to the orientation of the CO$_2$ approach transoid to the NO ligand of **3a,b**. The orange **4a,b(trans)** complexes could be

isolated in pure form in quantitative yields. Monitoring the CO$_2$ addition reactions visually, a purple color appeared indicating the presence of short-lived intermediates, which were not isolable and are proposed to be charge transfer complexes. This type of reaction of CO$_2$ with **3a,b** to form carbamates **4a,b-(trans)** is closely related to the 2 + 2 cycloaddition reactions of early transition metal imido complexes with alkynes, olefins and ketones.[26] Hessen and coworkers demonstrated an example of a thermodynamically favored insertion of alkynes into the V–amide bond of cationic amido imido vanadium complexes rather than a 2 + 2 cycloaddition reaction.[27] Therefore, an insertion reaction of CO$_2$ across the M–amide bond could alternatively be envisaged. Nevertheless, this CO$_2$ activation product is unique in its structure and is therefore in its way of formation presumed to be distinct from the insertion reactions of early transition M–N bonds.

The ^{31}P{^{1}H} NMR spectra of **4a,b(trans)** at room temperature exhibited sharp singlets at δ 61.9 and 56.4 ppm, respectively, indicating equivalence of the phosphorus atoms of the metal attached PNP ligand and under the given conditions also the absence of the theoretically possible isomeric products **4a,b(cis)** with the CO$_2$ approach from the NO side of **3a,b**. When the reactions of **3a,b** with CO$_2$ (2 bar) were carried out at −60 °C and pursued by ^{31}P{^{1}H} NMR spectroscopy, additional weak signals were seen at δ 62.7 and at 57.9 ppm besides those of **4a,b(trans)** indicating formation of kinetic mixtures of the **4a,b(trans,cis)** isomers (7 : 3 ratios in both cases of compounds). These mixtures equilibrated at room temperature into the thermodynamically more stable **4a,b-(trans)** as the sole products based on the reversibility of the CO$_2$ additions to **3a,b** from the NO side. **4a,b(cis)** could thus not be observed by ^{31}P{^{1}H} NMR spectroscopy at room temperature in solution and could also not be isolated (Scheme 2).

The ^{1}H NMR spectra of **4a,b(trans)** showed several distinct signals for the methyl, methylene and methyne protons in the expected region supporting also the absence of isomers. The IR spectra of **4a,b(trans)** displayed ν(NO) and ν(CO) bands at 1593, 1554 cm^{-1} and at 1902, 1879 cm^{-1}, respectively. Additional strong absorptions appeared for **4a,b(trans)** at 1732 and 1741 cm^{-1}, respectively, and were assigned to the ν_{CO_2} vibration of the attached CO$_2$ molecule. In the ^{13}C{^{1}H} NMR spectra of **4a,b(trans)** sharp singlets at δ 156.4 and 159.3 ppm were attributed to the C$_{CO_2}$ atoms along with multiplets at δ 247 and 250.6 ppm for the C$_{CO}$ atoms of the carbonyl ligands.

The C$_{CH_2}$ atoms adjacent to the nitrogen atoms of the PNP ligand of **4a,b(trans)** were observed as virtual triplets at δ 53.2 (t, $^v J_{CP}$ = 3.6 Hz) and at 57.7 (t, $^v J_{C-P}$ = 3.6 Hz) ppm, respectively. Single crystals of **4b(trans)** suitable for an X-ray diffraction study were obtained by layering pentane over a concentrated THF solution. The structural model obtained from the diffraction study is depicted in Fig. 5, which revealed a pseudo octahedral geometry. The W1–N2 bond distance was found to be 2.2603(19) Å. Upon CO$_2$ addition it became significantly elongated by about 0.2 Å with respect to the approximate W=N bond of **3b**.[23a]
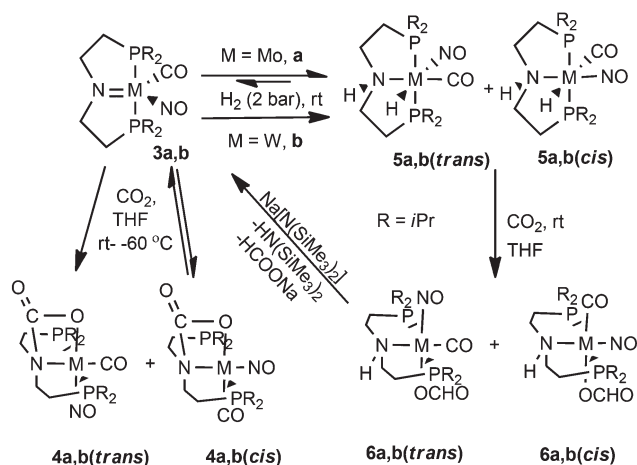
Scheme 2 CO$_2$ activation by molybdenum and tungsten amides **3a,b** and hydrides **5a,b(cis,trans)**.
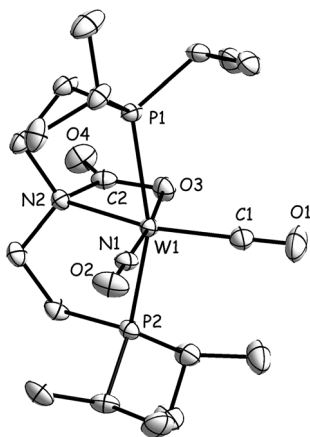
Fig. 5 Molecular structure of **4b**(*trans*). Thermal ellipsoids are drawn at the 50% probability level. All hydrogen atoms are omitted for clarity. Selected bond distances [Å] and bond angles [°]: W1–N1 1.789(2), W1–C1 1.969(3), W1–N2 2.2603(19), W1–O3 2.2155(18), C1–O1 1.159(3), C2–O3 1.283(3), C2–O4 1.208(3), N1–W1–C1 88.61(10), N2–W1–O3 172.47(8), N2–C2–O3 108.0 (2) P1–W1–P2 157.60(2).

The transition state of the reaction between W(NO)(CO)(PNP) **3b** and CO_2 could be modelled by DFT calculations (see ESI†).

Reasonably low activation energies $\Delta G^{\ddagger} = 14.4$ kcal mol^{-1} and 14.1 kcal mol^{-1} were calculated for the CO and NO side approaches of CO_2 onto **3b** to give **4b**(*trans*) and **4b**(*cis*), respectively. Remarkably, both approaches are kinetically almost not distinct. The free enthalpies of both reactions were determined to be −7.7 kcal mol^{-1} (**4b**(*trans*)) and −5.6 kcal mol^{-1} (**4b**(*cis*)) indicating that **4b**(*trans*) is the thermodynamically more favored and stable product. The calculated lower free energy value for **4b**(*cis*) looks plausible in view of the fact that the CO_2 approaches from the NO side are experimentally equilibria. The calculated activation barrier for the reverse reaction from **4b**(*cis*) to form **3b** and CO_2 seems thus to be still in energetic reach for a thermal process at room temperature ($\Delta G = 19.8$ kcal mol^{-1}). Drawings of the TS structure of the CO_2 approach to **3b** (Fig. 6 (left)) and the HOMO of the TS (Fig. 6 (right)) are shown in Fig. 6 (see also ESI†). According to the calculations the TS consists of a strongly distorted TS
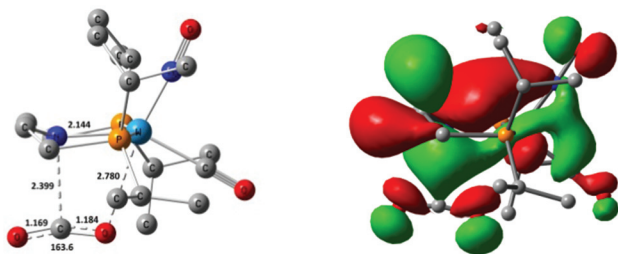
square with W–N, N–C, C–O and O–W contact lengths of 2.144, 2.399, 1.184 and 2.780 Å, respectively. These bond lengths mark an early transition state of the 2e + 2e reaction. The C–N interaction is the main new contact in the transition state, which is also represented in Fig. 6 (right), where large orbital coefficients appear between the C(CO_2) and the N atoms. The other new contact of the O(CO_2) atom to the W center is still very distant. Despite this feature that asymmetry prevails in the bond forming process, the reaction coordinate was found to be continuous and not two-stage without intermediate generated by consecutive bond formations.

Reactivity of the hydride complexes M(NO)H(CO)(PN^{H}P) (M = Mo, 5a(*cis,trans*); W, 5b(*cis,trans*)) with CO_2

Then we also tested the CO_2 reactivity of the previously reported[23a] isomeric mixtures of the amine hydride compounds M(NO)H(CO)(PN^{H}P) (**5a,b**(*cis,trans*)), which were obtained by H_2 addition to **3a,b** from both sides of the M≡N bond. The *cis* and *trans* notation indicate *trans* and *cis* attack of the H_2 molecule with respect to the NO ligand leading to the *trans* H/NO complexes (**5a,b**(*trans*)) or to the *trans* H/CO complexes (**5a,b**(*cis*)). However, the reactions to **5a**(*cis,trans*) with H_2 were found to be equilibria showing at room temperature an approximate 1 : 1 : 1 mixture of **5a**(*cis*)/**5a**(*trans*)/**3a**. Therefore, the reaction with CO_2 (2 bar) had to be carried out using the *in situ* generated mixture of Mo(NO)H(CO)(PN^{H}P) (**5a**(*cis, trans*)), which led to the formate products Mo(NO)(CO)(PN^{H}P) (η^1-OCHO) **6a**(*cis,trans*) and the cyclic carbamate species **4a**(*trans*) in an approx. 1 : 1 : 1 ratio as indicated by $^{13}C\{^1H\}$ and $^{31}P\{^1H\}$ NMR spectroscopy (Scheme 2). Since the three different kinds of reactions (2 kinds of CO_2 insertions into the M–H bonds and CO_2 addition) did not reveal a change in the ratios from the starting materials to the products, we have to assume that all involved reaction rates are about the same. The formate protons of **6a**(*trans*) and **6a**(*cis*) appeared in the ^1H NMR spectrum at δ 8.1 and 8.5 ppm, respectively (1 : 1 ratio). Signals at δ 170 and 168 ppm in the $^{13}C\{^1H\}$ NMR spectra were assigned to the $C_{formate}$ nuclei of the **6a**(*cis,trans*) isomers, respectively. **6a**(*cis,trans*) and **4a**(*trans*) were not in equilibrium, but despite this attempts to separate these complexes turned out to be unsuccessful.

Similarly, the reaction of the **5b**(*cis,trans*) mixture, which is not an equilibrium reaction allowing this mixture to be isolated, with CO_2 resulted at room temperature in the rapid formation of the isomeric η^1-formate complexes W(NO)(CO)(PN^{H}P)(η^1-OCHO) (**6a,b**(*trans*))[28] (Scheme 2) appearing in a 9 : 1 ratio. A strong signal at δ 51.3 ppm (with tungsten satellites) in the $^{31}P\{^1H\}$ NMR spectrum was assigned to **6b**(*trans*) along with a weak signal at δ 52.6 ppm for **6b**(*cis*). In the ^1H NMR spectrum the formate protons of **6b**(*trans,cis*) were observed at δ 8.5 and 8.0 ppm, respectively, and signals at δ 244.7 and 164.3 ppm in the $^{13}C\{^1H\}$ NMR spectra were attributed to the carbonyl ligand and the $C_{formate}$ atom of the major isomer **6b**(*trans*). Supposedly due to a too low concentration of **6b**(*cis*), the ^{13}C NMR resonances of the carbonyl and formate carbon atoms of the minor **6b**(*cis*) isomer could not be

Fig. 6 Geometry of the transition state (TS) of the approach of CO_2 to **3b** (left) and the TS HOMO−3 orbital for the CO_2 2e + 2e addition reaction (right).

observed. In the IR spectrum of the **6b(cis,trans)** mixture a band at 1612 cm^{-1} was attributed to the $\nu_{as}(CO_2)$ vibration in accord with earlier assignments of η^1-O-formato tungsten complexes.[28] Additional IR bands at 1863 and 1578 cm^{-1} of the **6b(cis,trans)** mixture were assigned to the $\nu(CO)$ and $\nu(NO)$ ligand vibrations of both compounds showing that both compounds cannot be distinguished in the 1500 to 1900 cm^{-1} region of the IR spectra.

Despite the fact that **6b(cis)** was the minor constituent of the isomeric mixture in solution, tiny crystals of this minor component could precipitated from solution by slow diffusion of pentane into a concentrated THF solution. The X-ray diffraction study revealed a pseudo-octahedral framework with *cis* nitrosyl and formate ligands (Fig. 7). The asymmetric unit of this minor isomer **6b(cis)** contained two crystallographically independent tungsten species displaying intermolecular hydrogen bonding[31] between the protic H_N atom of one molecule and the $O_{formato}$ of an adjacent molecule forming linear chains in the three dimensional lattice. It should be noted here that the H_N atom and the formate group were found to be disposed *anti* in the solid state structure, which was somewhat surprising when *cis* addition of H_2 to **3a,b** is taken into consideration, followed by CO_2 insertion into the M–H bond occurring with retention of the configuration at the metal centers (Scheme 2). One possible reason for the thermodynamically favored re-orientation of the H_N atom by a prototropic rearrangement could be the adoption of an energetically preferred intermolecular hydrogen bonding network requiring *anti* disposition of the H_N atom and the formate ligand in the crystal lattice.

In addition to these findings DFT calculations support the observation that the major *trans* NO/formate isomer **6b(trans)** is thermodynamically more stable than the *trans* CO/formate

isomer **6b(cis)** by $\Delta E = -4.4$ kcal mol^{-1} (see Scheme 2 and ESI†), which seems to match well reality. The fact that in the crystallization experiment of the **6b(cis,trans)** mixture **6b(cis)** was found to be less soluble than **6b(trans)** can now be attributed to a secondary crystallization effect based on the mentioned hydrogen bonding system in the solid state causing lower solubility of the minor constituent in solution. In addition it should be noted that the proton at N1 and the formate ligand of the structure of **6b(cis)** are in *anti* position, which somewhat contradicts the fact that in **5a,b(trans)** and **5a,b(cis)** they are expected to be *syn* due to the *Z* stereochemistry of the H_2 addition and the expected retention of the configuration at the metal center associated with the CO_2 insertion process. Therefore the proton at N1 is assumed to have undergone an inversion process when forming the crystals of **6b(cis)**, which seems likely on the basis of our DFT calculations, which revealed only minor energetic differences (approx. 2 kcal mol^{-1}) between the *syn* and *anti* structures in favour of the *anti* arrangements.

Stoichiometric hydrogenation of carbon dioxide

The **6a,b(cis,trans)** mixtures can be deprotonated at the H_N atom employing 1 equiv. of $Na[N(SiMe_3)_2]$ at room temperature with regeneration of **3a,b**. Sodium formate was formed in addition in accord with eqn (1) closing thus a stoichiometric cycle of consecutive reaction steps of H_2 and CO_2 additions in a "pseudo-catalytic" reaction course. The permanent presence of a base seemed not to interfere with **6b(cis,trans)** and to initiate side reactions, but the preferential addition of CO_2 over the H_2 addition to **3a,b** seemed in the presence of a H_2–CO_2 mixture a great obstacle to establish a genuine catalytic reaction course. Therefore, if catalysis should be accomplishable, it could be envisaged at higher temperatures making the CO_2 addition to some extent reversible enabling thus under catalytic conditions H_2 before CO_2 addition to **3a,b** (Scheme 3).

Being aware of this situation, we attempted catalysis and carried out at 140 °C 3 types of hydrogenation experiments of CO_2 applying the simultaneous presence of H_2 (70 bar) and CO_2 (10 bar) and of catalytic amounts of **3a,b** or of the **5b-(cis,trans)** mixture (5 mol% loading) in the presence of $Na[N(SiMe_3)_2]$ as stoichiometric agent. After 15 h all the experiments revealed formation of HCOONa according to eqn (1), but the yields were low, only 4%, 2% and 3%, respectively, as examined by ^1H NMR (DMF as internal standard) (Table 1). To improve the yield of the formate salt, we varied the type of the base using DBU, KOtBu or NEt$_3$ in the presence of **3a** as a catalyst with otherwise the same conditions as above. However, the yield of the formate salts [HCOO][DBUH] (3.5%), HCOOK (2.5%) or HCOOH–NEt$_3$ (0.5%), did not increase (Table 1). Furthermore, the addition of $B(C_6F_5)_3$ or the Et_3SiH–$B(C_6F_5)_3$ mixture as co-catalysts led in the presence of **3a** and $Na[N(SiMe_3)_2]$ even to a decrease in yields.

At this stage it can be stated that CO_2 hydrogenation is in principle possible, but for effective such catalyses further tuning efforts have to be taken into consideration, presumably
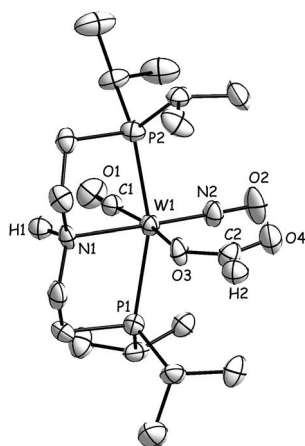
Fig. 7 Molecular structure of **6b(cis)**. Thermal ellipsoids are drawn at the 50% probability level. All hydrogen atoms are omitted for clarity except H1. Selected bond distances [Å] and bond angles [°]: W1–N1 2.287(5), W1–C1 1.930(8), W1–N2 1.792(6), W1–O3 2.185(5), C1–O1 1.172(8), C2–O3 1.271(7), C2–O4 1.213(8), N1–W1–C1 91.6(3), N2–W1–O3 101.9(2), N1–W1–N2 178.3 (3) P1–W1–P2 158.32(7).
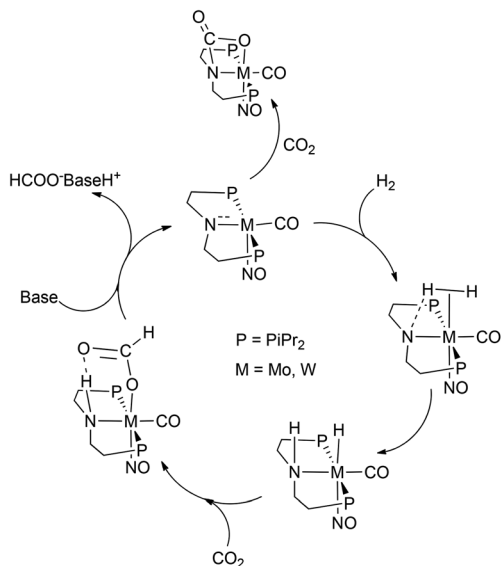
Scheme 3 Schematic cycle for the CO_2 hydrogenation using **3a,b**.

Table 1 Hydrogenation of CO_2

$$CO_2 + H_2 + Na[N(SiMe_3)_2] \xrightarrow[140\,°C, THF]{cat\,(5\,mol\%)} HCOONa + HN(SiMe_3)_2 \quad (1)$$
$$\;_{(10\,bar)}\;_{(70\,bar)}$$

Entry[a]	Cat	Base	Time (h)	Yield[b] (%)
1	**3a**	$Na[N(SiMe_3)_2]$	15	4
2	**3b**	$Na[N(SiMe_3)_2]$	15	2
3	**5b**(*cis,trans*)	$Na[N(SiMe_3)_2]$	15	3
4	**3a**	DBU	15	3.5
5	**3a**	KO*t*Bu	15	2.5
6	**3a**	Et_3N	15	0.50
7[c]	—	$Na[N(SiMe_3)_2]$	17	0.14
8	**3a**	TMP	15	—
9	**3a**/BCF	$Na[N(SiMe_3)_2]$	15	0.70
10	**3a**/Et_3SiH/BCF	$Na[N(SiMe_3)_2]$	22	0.30

[a] Unless and otherwise stated 10 bar CO_2, 70 bar H_2, THF as solvent, 140 °C temperature and 5 mol% catalyst with respect to base were used as reaction conditions. [b] Yield on the basis of ^{1}H NMR integration using DMF as internal standard. [c] No catalyst was used.

by attempts to make the CO_2 adducts of type **4** more labile. It should be mentioned at this point that since strong bases are known to react with CO_2 particularly at high temperatures and pressures, a control experiment was also carried out in the absence of the metal catalyst applying only $Na[N(SiMe_3)_2]$ as the catalyst and keeping all the other conditions the same. The yield of sodium formate was in this case only 0.14%, which is significantly lower than the yields obtained in the presence of **3a,b**.

It deserves mentioning that after the CO_2 hydrogenation experiments (applying especially the $NaN(SiMe_3)_2$ base), the reaction mixtures were found to contain a considerable amount of white precipitate in the THF reaction mixture. When THF was evaporated *in vacuo* and the residue was dissolved in D_2O to quantify the yield of the formate salt by [1]H

NMR spectroscopy (DMF internal standard), the solution was still found to contain white particles even after addition of excess D_2O. Therefore, formation of another species is anticipated to be produced in the hydrogenation of CO_2 (note that the product sodium formate is expected to be soluble in D_2O). The nature of this species could however not be unravelled, but in principle it should be added to the overall yield of these catalytic reactions.

Conclusions

In conclusion we have reported a new synthetic route for the preparation of isomeric diamagnetic $M(NO)Cl_3(PN^HP)$ (M = Mo, **1a**(*syn,anti*); W, **1b**(*syn,anti*)) complexes and their reduction to rare paramagnetic species $M(NO)Cl_2(PN^HP)$ {M = Mo, **2a**(*syn,anti*); W, **2b**(*syn,anti*)}. Furthermore, we have shown that the excessively reduced pentacoordinate amides Mo,W(0)(PNP)(NO)(CO) (**3a,b**; PNP = $(iPr_2PCH_2CH_2)_2N$)) can activate CO_2 in a metal–ligand assisted way *via* 2e + 2e additions across the M=N bonds forming the pseudo-octa-hedral **4a,b**(*trans*) compounds. The CO_2 approach occurs thermodynamically controlled from the CO ligand side. Kinetically there is practically no distinction between the sides of attack. The amine hydride species $M(NO)(CO)H(PN^HP)$ (M = Mo, **5a**-(*cis,trans*) W, **5b**(*cis,trans*)) formed by H_2 addition to **3a,b** reacted with CO_2 at room temperature to produce η^1-formato complexes $M(NO)(CO)(PN^HP)(\eta^1\text{-}OCHO)$ {M = Mo, **6a**(*cis,trans*); W, **6b**(*cis,trans*)}. Stoichiometric hydrogenations of CO_2 to formate salts could thus be accomplished *via* elimination of the formate ligands of type **6** complexes induced through the presence of a strong base regenerating the amides **3a,b**. Catalytic hydrogenation of CO_2 was then also approached at somewhat elevated temperatures and pressures. However, the apparently too high stability of the CO_2 addition products of type **4** are anticipated to largely block the catalytic reaction course and cause low yields. This conclusion rendered the idea that in these Mo and W systems catalysis could eventually be achieved by tuning the **4** type complexes for reversibility in CO_2 additions. It is finally worth mentioning that this study demonstrated for the first time that reductions of CO_2 are within reach utilizing middle, non-noble transition metal compounds as catalysts.

Experimental section

General procedures

All experiments were carried out under an atmosphere of nitrogen using either dry glove box or Schlenk techniques. Reagent grade solvents benzene, tetrahydrofuran, pentane, toluene, diethyl ether were dried with sodium benzophenone and distilled prior to use under N_2 atmosphere. CH_2Cl_2 and Et_3N were dried over calcium hydride and distilled. Deuterated solvents were dried with sodium benzophenone ketyl (THF-d_8, toluene-d_8 and C_6D_6) and calcium hydride (CD_2Cl_2) and distilled

via freeze–pump–thaw cycle prior to use. The M(NO)-Cl$_3$(NCMe)$_2$,[29] M(NO)(CO)(PNP),[23a] {M = Mo, W; PNP = N(CH$_2$CH$_2$iPr$_2$)$_2$} complexes and HN(CH$_2$CH$_2$^{i}Pr$_2$)$_2$[30] were prepared according to literature procedures. KOtBu, Na[N(SiMe$_3$)$_2$] and DBU were purchased from commercially available sources and used without further purification. The NMR spectra were measured with a Varian Mercury 200 spectrometer (at 200.1 MHz for ^{1}H, at 81.0 MHz for ^{31}P), with Varian Gemini-300 instrument (^{1}H at 300.1 MHz, ^{13}C at 75.4 MHz), with Bruker-DRX 500 spectrometer (500.2 MHz for ^{1}H, 202.5 MHz for ^{31}P, 125.8 MHz for ^{13}C) and Bruker-DRX 400 spectrometer (400.1 MHz for ^{1}H, 162.0 MHz for ^{31}P, 100.6 MHz for ^{13}C). All chemical shifts for ^{1}H and ^{13}C{^{1}H} are expressed in ppm relative to tetramethylsilane (TMS) and for ^{31}P{^{1}H} relative to 85% H$_3$PO$_4$ as an external standard reference. Signal patterns are as followed: s, singlet; d, doublet; t, triplet; q, quartet; m, multiplet; v, virtual triplet. IR spectra were obtained either ATR or KBr methods using Bio-rad FTS-45 instrument. Elemental analyses were carried out at Anorganisch-Chemisches Institut of the University of Zurich.

Preparation of isomeric mixture of Mo(NO)Cl$_3$(PN^{H}P), 1a(*syn,anti*)

To a solution of Mo(NO)Cl$_3$(NCMe)$_2$ (0.200 g, 0.636 mmol) in 10 mL of THF, 0.16 g (196 mg, 0.64 mmol) (iPr$_2$PCH$_2$CH$_2$)$_2$NH ligand in 5 mL THF was added. The resulting mixture was kept stirring overnight to obtain a light green precipitate and the solution becomes dark green. Then the solvent was separated from the precipitate and the precipitate was washed with minimum amount of THF and extracted with dichloromethane and dried *in vacuo* to obtain the powdery isomeric mixture of 1a(*syn,anti*) in 55% yield.

^{1}H NMR (400 MHz, CD$_2$Cl$_2$): δ = 4.4 (broad singlet, NH, 1a(*syn*)), 3.63–3.5 (m, NCH$_2$), 3.23–3.21 (m, NCH$_2$), 3.1–3.02 (m, CH), 2.3–2.2 (m, –PCH$_2$), 2.05 (m, PCH$_2$), 1.52–1.39 (m, CH$_3$, 1a(*syn*)), 1.34–1.30 (m, CH$_3$, 1a(*anti*)). ^{13}C{^{1}H} NMR (100.6 MHz, CD$_2$Cl$_2$): δ = 55.9 (t, ^{v}J$_{C-P}$ = 3.6 Hz, NCH$_2$, 1a(*syn*)), 29 (m, CH), 28 (m, PCH$_2$), 21 (m, CH$_3$), 20.4 (m, CH$_3$). ^{31}P{^{1}H} NMR (400 MHz, CD$_2$Cl$_2$): 69.3 (s, ^{i}Pr$_2$P, 1a(*syn*)), 71 (s, 1a(*anti*)). IR (cm^{-1}, ATR): 1653 (ν_{NO}), expected *m/z*: 538, observed *m/z*: 538.2. Anal. Calcd for C$_{16}$H$_{37}$Cl$_3$MoN$_2$OP$_2$: C, 35.74; H, 6.94; N, 5.21. Found: C, 36.03; H, 6.39; N, 5.67.

Preparation of isomeric mixture of W(NO)Cl$_3$(PN^{H}P), 1b(*syn,anti*)

WCl$_3$(NO)(NCMe)$_2$ (200 mg, 0.5 mmol) was dissolved in 10 mL of THF. 0.160 g (0.52 mmol) of aminodiphosphine (iPr$_2$PCH$_2$CH$_2$)$_2$NH was added *via* a syringe. After a few minutes stirring a light red precipitate was observed and the reaction was allowed to stir overnight. Then the solution was removed partially under vacuum and the reddish residue was filtered off and washed with THF. The obtained residue was extracted with dichloromethane and the solvent was removed *in vacuo* to obtained the isomeric mixture of 1b(*syn,anti*) in 62% yield. ^{1}H NMR (400 MHz, CD$_2$Cl$_2$): δ = 4.47 (broad singlet, NH, 1b(*syn*)), 5.5 (broad singlet, NH, 1b(*anti*)) 3.71–3.57 (m,

NCH$_2$, *syn,anti*), 3.19–3.05 (m, CH), 2.30–2.23 (m, –PCH$_2$), 2.09–2.06 (m, PCH$_2$), 1.47–1.19 (m, CH$_3$). ^{13}C{^{1}H} NMR (100.6 MHz, CD$_2$Cl$_2$): δ = 55.9 (t, ^{v}J$_{C-P}$ = 5.9 Hz, NCH$_2$, 1b(*anti*)), 55 (t, ^{v}J$_{C-P}$ = 4.8 Hz, NCH$_2$, 1b(*anti*)), 27.8 (m, CH), 27.3 (m, –PCH$_2$), 20 (m, CH$_3$). ^{31}P{^{1}H} NMR (400 MHz, CD$_2$Cl$_2$): 56.8 [s, ^{1}J$_{P-W}$ (d, satellite) = 184.8 Hz, 1b(*syn*)], 58.3 [s, ^{1}J$_{P-W}$ (d, satellite) = 189.3 Hz, 1b(*anti*)]. IR (cm^{-1}, ATR): 1596 (ν_{NO}), Anal. Calcd for C$_{16}$H$_{37}$Cl$_3$N$_2$OP$_2$W: C, 30.72; H, 5.96; N, 4.48. Found: C, 30.72; H, 5.88; N, 4.55.

Preparation of Mo(NO)Cl$_2$(PN^{H}P), 2a(*syn,anti*)

The isomeric mixture of 1a(*syn,anti*) (0.030 g, 0.056 mmol) was added to a stirred suspension of approximately 1% sodium amalgam (0.0013 g, 0.057 mmol) in 15 mL THF. Stirring was continued overnight at room temperature to ensure the completion of the reaction. The final supernatant green solution was filtered off from the mercury containing residue and evaporated to dryness. The resulting residue was washed with pentane and extracted with THF. Finally the isomeric mixture of 2a(*syn,anti*) was obtained as a green powder after removal of THF *in vacuo*. Yield 74%. IR (cm^{-1}, ATR): 1595 (ν_{NO}), Anal. Calcd for C$_{16}$H$_{37}$Cl$_2$MoN$_2$OP$_2$: C, 38.26; H, 7.42; N, 5.58. Found: C, 37.88; H, 7.12; N, 5.29.

Preparation of W(NO)Cl$_2$(PN^{H}P), 2b(*syn,anti*)

0.075 g (0.12 mmol) of the isomeric mixture of 1b(*syn,anti*) was added to a stirred suspension of 1% sodium amalgam (0.003 g, 0.13 mmol) in 15 mL THF. Stirring was continued overnight at room temperature to ensure the completion of the reaction. The final supernatant solution was filtered off from the mercury containing residue and evaporated to dryness. The residue was washed with pentane and extracted with THF and later with toluene. Recrystallisation from cold toluene–pentane solution afforded green crystals of 2b(*syn,anti*). Yield 78%. IR (cm^{-1}, ATR): 1547 (ν_{NO}). Anal. Calcd for W(NO)Cl$_2$(PNP): C, 32.56; H, 6.32; N, 4.75. Found: C, 32.71; H, 6.22; N, 4.78.

General procedure for the preparation of M(NO)(CO)(PNP)(OCO), (M = Mo, 4a(*trans*); W, 4b(*trans*))

M(NO)(CO)(PNP) (0.065 mmol, M = Mo, 3a; W, 3b) was dissolved in 0.5 mL THF-d_8 in a J. Young NMR tube. The tube was taken out from the glove box and frozen with liquid nitrogen. The nitrogen atmosphere was removed *via* a freeze–pump–thaw cycle and the tube was filled with 2 bar of CO$_2$ and sealed. Formation of 4a(*trans*) or 4b(*trans*) took place immediately within five minutes in quantitative yield.

4a(*trans*). ^{1}H NMR (400 MHz, THF-d_8): δ = 3.47–3.35 (m, 2H, –NCH$_2$), 2.85–2.78 (m, 2H, –NCH$_2$), 2.42–2.36 (m, 2H, CH), 2.25–2.17(m, 2H, CH), 2.08–2.03 (m, 2H, CH$_2$), 1.81–1.72 (m, 2H, –PCH$_2$), 1.35–1.28 (m, 12H, CH$_3$), 1.23–1.15 (m, 12H, CH$_3$). ^{13}C{^{1}H} NMR (100.62 MHz THF-d_8): δ = 247 (m, CO), 156.4 (s, CO$_2$), 53.2 (t, ^{v}J$_{CP}$ = 3.6 Hz, NCH$_2$), 23.79 (s, CH), 19.83 (t, ^{v}J$_{C-P}$ = 6 Hz, CH$_2$), 16.59 (s, CH$_3$), 16.21 (s, CH$_3$), 15.74 (s, CH$_3$). ^{31}P{^{1}H} NMR (161.97 MHz, THF-d_8): δ = 61.9 (s). IR (cm^{-1}, KBr): 1593 (ν_{NO}), 1732 (ν_{CO}), 1902 (ν_{CO}). Anal. Calcd for

$C_{18}H_{36}MoN_2O_4P_2$: C, 43.03; H, 7.22; N, 5.58. Found: C, 42.67; H, 7.28; N, 5.34.

4b(trans). ^{1}H NMR (400 MHz, THF-d_8): δ = 3.58–3.49 (m, 2H, –NCH$_2$), 2.92–2.85 (m, 2H, –NCH$_2$), 2.52–2.46 (m, 2H, CH), 2.28–2.20 (m, 2H, CH), 2.11–2.06 (m, 2H, –PCH$_2$), 1.81–1.76 (m, 2H, –PCH$_2$), 1.37–1.29 (m, 12H, –CH$_3$), 1.25–1.11 (m, 12H, –CH$_3$). ^{13}C{^{1}H} NMR (75.45 MHz, THF-d_8): δ = 250.6 (m, CO), 159.3 (s, CO$_2$), 57.7 (t, $^vJ_{C–P}$ = 3.6 Hz, NCH$_2$), 27.53 (t, $^vJ_{CP}$ = 10.9 Hz, CH), 26.87 (t, $^vJ_{CP}$ = 12.2 Hz, CH), 23.62 (t, $^vJ_{CP}$ = 7.7 Hz, PCH$_2$), 19.66 (t, $^vJ_{CP}$ = 5.9 Hz, CH$_3$), 19.05 (s, CH$_3$), 18.61 (s, CH$_3$). ^{31}P{^{1}H} NMR (161.97 MHz, THF-d_8): 56.4 [s, $^1J_{PW}$ (d, satellite) = 308.2 Hz]. IR (cm^{-1}, KBr): 1554 (ν_{NO}), 1741 (ν_{CO_2}), 1879 (ν_{CO}). Anal. Calcd for $C_{18}H_{36}N_2O_4P_2W$: C, 36.63; H, 6.15; N, 4.75. Found: C, 36.29; H, 6.27; N, 4.72.

Reaction of 3a and 3b with CO$_2$ at 213 K. M(NO)(CO)(PNP) (0.03 mmol) (M = Mo, **3a**; W; **3b**) was dissolved in 0.5 mL THF-d_8 in a J. Young NMR tube. The tube was taken out of the glove box and frozen with liquid nitrogen. The nitrogen atmosphere was removed *via* freeze–pump–thaw cycle. The tube was filled with 2 bar of CO$_2$ under frozen condition and sealed. Then the tube was immediately placed in a 300 MHz NMR spectrometer preset at −60 °C and ^{31}P{^{1}H} NMR spectra was recorded.

^{31}P{^{1}H} NMR data for the reaction of **3a** with CO$_2$ at 213 K: ^{31}P{^{1}H} NMR (121.48 MHz, 213 K, THF-d_8): δ = 63.1 (s, formation of **4a(trans)**), 62.7 (s, formation of **4a(cis)**).

^{31}P{^{1}H} NMR data for the reaction of **3b** with CO$_2$ at 213 K: ^{31}P{^{1}H} NMR (121.48 MHz, 213 K, THF-d_8): δ = 58.1 (s, formation of **4b(trans)**), 57.9 (s, formation of **4b(cis)**).

Preparation of Mo(NO)(CO)(PN^{H}P)(η^1-OCHO), {mixture of 6a(cis) and 6a(trans)}. **3a** (0.015 g, 0.033 mmol) in 0.5 mL THF was frozen in a J. Young NMR tube. The nitrogen atmosphere was removed *via* a freeze–pump–thaw cycle. Then the tube was filled with 2 bar of H$_2$ and sealed and kept for three days to allow formation of **5a(cis)** and **5a(trans)**. After formation of the equilibrium mixture of hydride complexes **5a(cis)** and **5a(trans)** along with **3a** (1 : 1 : 1), the hydrogen pressure was slowly released and CO$_2$ (2 bar) was purged into that mixture instantaneously. Immediate formation of **6a(cis)** and **6a(trans)** was observed along with **4a(trans)** in a ratio of 1 : 1 : 1 as revealed by the ^{31}P{^{1}H} NMR.

Selected spectroscopic data: ^{1}H NMR (400.1 MHz, THF-d_8) data: δ = 8.5 (s, 1H, OCH, **6a(cis)**), 8.1 (s, 1H, OCHO, **6a(trans)**). ^{13}C{^{1}H} NMR (100.6 MHz, THF-d_8): δ 248 (s, CO, **6a(trans)**), 246.5 (s, CO, **6a(cis)**), 170 (s, OCHO, **6a(cis)**), 168.8 (s, OCHO, **6a(trans)**), 156 (s, CO$_2$, **4a(trans)**). ^{31}P{^{1}H} NMR (161.97 MHz, THF-d_8): 60.9 (s, **6a(trans)**), 60.0 (s, **6b(cis)**). Since the resulting product contains mixtures of **6a(cis)**, **6a(trans)** and **4a(trans)** which could not be separated, elemental analyses could not be provided.

W(NO)(CO)(PN^{H}P)(η^1-OCHO), {mixture of 6b(cis) and 6b-(trans)}. A solution of the mixture of **5b(cis)** and **5b(trans)** (0.020 g, 0.036 mmol) in 0.5 mL THF was frozen in a J. Young NMR tube. The nitrogen atmosphere was removed *via* a freeze–pump–thaw cycle. Then the tube was filled with 2 bar of CO$_2$ and sealed. Formation of **6b(cis)** and **6b(trans)** took place

immediately upon shaking the Young NMR tube in quantitative yield in a 1 : 9 ratio. Suitable orange crystals were obtained for diffraction upon layering pentane to a concentrated THF solution of the product. Yield (by ^{31}P{^{1}H} NMR): 10% (**6b(cis)**), 90% (**6b(trans)**). ^{1}H NMR (400.1 MHz, THF-d_8): δ = 8.52 (s, 1H, OCH, **6b(trans)**), 8.0 (s, 1H, OCH, **6b(cis)**), 2.93 (m, 4H, –NCH$_2$), 2.41–2.26 (m, 4H, –CH), 1.66–1.62 (m, 4H, CH$_2$P), 1.35–1.25 (m, 24H, CH$_3$). ^{13}C{^{1}H} NMR (100.6 MHz, THF-d_8): δ 244.7 (s, CO), 164.3 (s, CO$_2$H), 57.7 (s, NCH$_2$), 24.5 (t, $^vJ_{CP}$ = 13.1 Hz, CH), 24.01 (t, $^vJ_{CP}$ = 9.5 Hz, CH), 19.08 (t, $^vJ_{CP}$ = 8.3 Hz, CH$_2$), 17.2 (s, CH$_3$), 14.80 (s, CH$_3$). ^{31}P{^{1}H} NMR (161.97 MHz, THF-d_8): 51.3 (s, **6b(trans)**), 52.6 (s, **6b(cis)**). IR (cm^{-1}, KBr): 1578 (ν_{NO}), 1612 (ν_{OCHO}), 1863 (ν_{CO}). Anal. Calcd for $C_{18}H_{38}N_2O_4P_2W$: C, 36.50; H, 6.47; N, 4.73. Found: C, 36.25; H, 6.41; N, 4.53.

General procedure for the reaction of the formate complexes (mixture of 6a(cis) and 6a(trans)) and (mixture of 6b(cis) and 6b(trans)) with Na[N(SiMe$_3$)$_2$]

The mixture of the formate complexes (0.03 mmol) of molybdenum (mixture of **6a(cis)** and **6a(trans)** along with **4b(trans)**) and tungsten (mixture of **6b(cis)** and **6b(trans)**) was dissolved in THF in a J. Young NMR tube. Then 1 equiv. of Na-[N(SiMe$_3$)$_2$] was added. The mixture was shaken vigorously. The ^{31}P{^{1}H} NMR spectra revealed immediate regeneration of **3a** or **3b**. Then the reaction mixture was dried *in vacuo* and extracted with pentane to remove the **3a** or **3b**. The remaining solid insoluble in pentane was dissolved in D$_2$O. The ^{1}H NMR spectra in D$_2$O revealed the formation of HCOONa.

General procedures for the CO$_2$ hydrogenations. A steel autoclave was charged under nitrogen with the catalysts (0.1 mmol, 5 mol% with respect to base) dissolved in 0.5 mL of THF and 20 equiv. of Na[N(SiMe$_3$)$_2$] (1 M in THF). The tube was pressurized with 40 bar H$_2$ and allowed to stir at room temperature for half an hour. After this period of time 10 bar of CO$_2$ was charged. Then the total pressure was kept at 80 bar filling with H$_2$ pressure. The reaction mixture was heated to 140 °C (Caution!!: pressure rises to 100 bar). After certain reaction times, the autoclave was cooled to room temperature and the pressure was released. The THF solvent was evaporated to dryness and D$_2$O was added to dissolve the solid residue. Dimethylformamide (2 µL) was added to the reaction mixtures as an internal standard for the determination of the yield by ^{1}H NMR spectroscopy. ^{1}H NMR (300 MHz, D$_2$O): δ = 8.3 (s, 1H, HCOONa).

X-ray diffraction analyses

The data collection and structure refinement data for **2a(anti)**, **2b(syn)**, **4b(trans)** and **6b(cis)** are presented in (Table 2). Single-crystal X-ray diffraction data were collected at 183(2) K on a Xcalibur diffractometer (Agilent Technologies, Ruby CCD detector) for all compounds using a single wavelength Enhance X-ray source with MoKα radiation (λ = 0.71073 Å).[32a] The selected suitable single crystals were mounted using poly-butene oil on the top of a glass fiber fixed on a goniometer head and immediately transferred to the diffractometer. Pre-

Table 2 Crystallographic data for compounds **2a(anti)**, **2b(syn)**, **4b(trans)** and **6b(cis)**[a]

	2a(anti)	2b(syn)	4b(trans)	6b(cis)
CCDC	960495	960496	888516	888517
Empirical formula	$C_{16}H_{37}Cl_2MoN_2OP_2$	$C_{16}H_{37}Cl_2N_2OP_2W$	$C_{18}H_{36}N_2O_4P_2W$	$8(C_{18}H_{38}N_2O_4P_2W), C_4H_8O$
Formula weight (g mol^{-1})	502.26	590.16	590.28	4810.46
Temperature (K)	183(2)	183(2)	183(2)	183(2)
Wavelength (Å)	0.71073	0.71073	0.71073	0.71073
Crystal system, space group	Orthorhombic, $P2_12_12_1$	Orthorhombic, $P2_12_12_1$	Monoclinic, $P2_1/c$	Tetragonal, $I4_1/a$
a (Å)	7.3971(1)	7.4129(1)	7.8847(1)	36.3651(6)
b (Å)	13.2575(2)	13.2003(2)	26.3644(4)	36.3651(6)
c (Å)	23.8535(4)	23.8800(5)	11.5872(2)	14.8550(3)
α (°)	90	90	90	90
β (°)	90	90	106.979(2)	90
γ (°)	90	90	90	90
Volume (Å^3)	2339.24(6)	2336.72(7)	2303.70(7)	19644.6(8)
Z, density (calcd) (Mg m^{-3})	4, 1.426	4, 1.678	4, 1.702	4, 1.626
Abs coefficient (mm^{-1})	0.933	5.316	5.178	4.859
$F(000)$	1044	1172	1176	9632
Crystal size (mm^3)	0.30 × 0.11 × 0.06	0.12 × 0.10 × 0.06	0.33 × 0.27 × 0.20	0.10 × 0.08 × 0.03
θ range (°)	2.88 to 32.58	2.88 to 28.28	2.70 to 28.28	2.44 to 25.68
Reflections collected	55 639	16 728	37 089	27 807
Reflections unique	8495/[R_{int} = 0.0485]	5804/[R_{int} = 0.0372]	5720/[R_{int} = 0.0263]	9319/[R_{int} = 0.0800]
Completeness to θ (%)	99.9	99.9	99.9	99.9
Absorption correction	Analytical	Analytical	Analytical	Analytical
Max/min transmission	0.951 and 0.799	0.765 and 0.644	0.432 and 0.275	0.995 and 0.987
Data/restraints/parameters	7529/0/225	5804/61/257	5574/0/252	5971/0/510
Goodness-of-fit on F^2	1.030	0.895	1.294	0.987
Final R_1 and wR_2 indices [$I > 2\sigma(I)$]	0.0351, 0.0852	0.0329, 0.0488	0.0203, 0.0400	0.0488, 0.0619
R_1 and wR_2 indices (all data)	0.0420, 0.0872	0.0473, 0.0505	0.0212, 0.0403	0.0972, 0.0744
Absolute structure parameter	−0.02(3)	−0.007(7)		
Largest diff. peak and hole (e Å^{-3})	1.107 and −0.613	2.044 and −1.158	0.657 and −1.231	1.241 and −0.845

[a] The unweighted R-factor is $R_1 = \sum(F_o - F_c)/\sum F_o$; $I > 2\sigma(I)$ and the weighted R-factor is $wR_2 = \{\sum w(F_o^2 - F_c^2)^2/\sum w(F_o^2)^2\}^{1/2}$.

experiment, data collection, data reduction and analytical absorption corrections[32b] were performed with the program suite CrysAlis^{Pro}.[32a] The crystal structures were solved with SHELXS97[32c] using direct methods. The structure refinements were performed by full-matrix least-squares on F^2 with SHELXL97.[32c] All programs used during the crystal structure determination process are included in the WINGX software.[32d] PLATON[32e] was used to check the result of the X-ray analyses and DIAMOND[32f] was used for the molecular graphics. CCDC 888516 (for **4b(trans)**), 888517 (for **6b(cis)**), 960495 (for **2a(anti)**) and 960496 (for **2b(syn)**) contain the supplementary crystallographic data (excluding structure factors) for this paper.

Acknowledgements

Notes and references

1 (a) *Carbon Dioxide as Chemical Feedstock*, ed. M. Aresta, Wiley-VCH, Weinheim, 2010; (b) M. Cokoja, C. Bruckmeier, B. Rieger, W. A. Herrmann and F. E. Kühn, *Angew. Chem., Int. Ed.*, 2011, **50**, 8510–8537.

2 (a) T. Sakakura, J.-C. Choi and H. Yasuda, *Chem. Rev.*, 2007, **107**, 2365–2387; (b) X. Yin and J. R. Moss, *Coord. Chem. Rev.*, 1999, **181**, 27–59.

3 (a) P. G. Jessop, T. Ikariya and R. Noyori, *Chem. Rev.*, 1995, **95**, 259–272; (b) P. G. Jessop, F. Joó and T. Chih-C, *Coord. Chem. Rev.*, 2004, **248**, 2425–2442; (c) W. Leitner, *Angew. Chem., Int. Ed. Engl.*, 1995, **34**, 2207–2221.

4 (a) C. Gunanathan and D. Milstein, *Acc. Chem. Res.*, 2011, **44**, 588–602; (b) M. D. Fryzuk and P. A. MacNeil, *Organometallics*, 1983, **2**, 682–684; (c) A. Friedrich, M. Drees, M. Käss, E. Herdtweck and S. Schneider, *Inorg. Chem.*, 2010, **49**, 5482–5494; (d) C. M. Fafard, D. Adhikari, B. M. Foxman, D. J. Mindiola and O. V. Ozerov, *J. Am. Chem. Soc.*, 2007, **129**, 10318–10319; (e) E. Khaskin, M. A. Iron, L. J. W. Shimon, J. Zhang and D. Milstein, *J. Am. Chem. Soc.*, 2010, **132**, 8542–8543; (f) C. Gunanathan, B. Gnanaprakasam, M. A. Iron, L. J. W. Shimon and D. Milstein, *J. Am. Chem. Soc.*, 2010, **132**, 14763–14765; (g) L. Schwartsburd, M. A. Iron, L. Konstantinovski, E. Ben Ari and D. Milstein, *Organometallics*, 2011, **30**, 2721–2729; (h) S. Kohl, L. Weiner, L. Schwartsburd, L. Konstantinovski, L. J. W. Shimon, Y. Ben-David, M. A. Iron and D. Milstein, *Science*, 2009, **324**, 74–77; (i) E. Ben-Ari, G. Leitus, L. J. W. Shimon and D. Milstein, *J. Am. Chem. Soc.*, 2006, **128**, 15390–15391.

5 (a) R. Noyori, M. Koizumi, D. Ishii and T. Ohkuma, *Pure Appl. Chem.*, 2001, **73**, 227–232; (b) S. Clapham, A. Hadzovic

and R. Morris, *Coord. Chem. Rev.*, 2004, **248**, 2201–2237; (*c*) T. Ikariya and A. J. Blacker, *Acc. Chem. Res.*, 2007, **40**, 1300–1308; (*d*) C. Gunanathan and D. Milstein, *Acc. Chem. Res.*, 2011, **44**, 588–602; (*e*) H. Grützmacher, *Angew. Chem., Int. Ed.*, 2008, **47**, 1814–1818; (*f*) Y. Blum, D. Czarkie, Y. Rahamim and Y. Shvo, *Organometallics*, 1985, **4**, 1459–1461.

6 C. A. Huff, J. W. Kampf and M. S. Sanford, *Organometallics*, 2012, **31**, 4643–4645.

7 (*a*) M. Vogt, M. Gargir, M. A. Iron, Y. Diskin-Posner, Y. Ben-David and D. Milstein, *Chem. – Eur. J.*, 2012, **18**, 9194–9197; (*b*) M. Vogt, A. Nerush, Y. Diskin-Posner, Y. Ben-David and D. Milstein, *Chem. Sci.*, 2014, **5**, 2043–2051.

8 (*a*) C. M. Mömming, E. Otten, G. Kehr, R. Frçhlich, S. Grimme, D. W. Stephan and G. Erker, *Angew. Chem., Int. Ed.*, 2009, **48**, 6643–6646; (*b*) A. E. Ashley, A. L. Thompson and D. O'Hare, *Angew. Chem., Int. Ed.*, 2009, **48**, 9839–9843; (*c*) G. Ménard and D. W. Stephan, *J. Am. Chem. Soc.*, 2010, **132**, 1796–1797; (*d*) J. Boudreau, M. A. Courtemanche and F. G. Fontaine, *Chem. Commun.*, 2011, **47**, 11131–11133; (*e*) L. J. Hounjet, C. B. Caputo and D. W. Stephan, *Angew. Chem., Int. Ed.*, 2012, **51**, 4714; (*f*) I. Peuser, R. C. Neu, X. Zhao, M. Ulrich, B. Schirmer, J. A. Tannert, G. Kehr, R. Fröhlich, S. Grimme, G. Erker and D. W. Stephan, *Chem. – Eur. J.*, 2011, **17**, 9640.

9 Y. Jiang, O. Blacque, T. Fox and H. Berke, *J. Am. Chem. Soc.*, 2013, **135**, 7751–7760.

10 J. F. Hull1, Y. Himeda, W.-H. Wang, B. Hashiguchi, R. Periana, D. J. Szalda, J. T. Muckerman and E. Fujita, *Nat. Chem.*, 2012, **4**, 383–388.

11 (*a*) C. Federsel, R. Jackstell and M. Beller, *Angew. Chem., Int. Ed.*, 2010, **49**, 6254–6257; (*b*) A. H. Chelsea and M. S. Sanford, *J. Am. Chem. Soc.*, 2011, **133**, 18122–18125.

12 (*a*) S. Wesselbaum, T. Vom Stein, J. Klankermayer and W. Leitner, *Angew. Chem., Int. Ed.*, 2012, **51**, 7499–7502; (*b*) M. J. Sgro and D. W. Stephan, *Angew. Chem., Int. Ed.*, 2012, **51**, 11343–11345.

13 P. G. Jessop, T. Ikariya and R. Noyori, *Nature*, 1994, **368**, 231–233.

14 P. G. Jessop, Y. Hsiao, T. Ikariya and R. Noyori, *J. Am. Chem. Soc.*, 1996, **118**, 344–355.

15 (*a*) F. Joó, G. Laurenczy, L. Nádasdi and J. Elek, *Chem. Commun.*, 1999, 971–972; (*b*) C. A. Huff and M. S. Sanford, *ACS Catal.*, 2013, **3**, 2412–2416.

16 E. Graf and W. Leitner, *J. Chem. Soc., Chem. Commun.*, 1992, 623–624.

17 F. Gassner and W. Leitner, *J. Chem. Soc., Chem. Commun.*, 1993, 1465–1466.

18 Y. Himeda, N. Onozawa-Komatsuzaki, H. Sugihara and K. Kasuga, *Organometallics*, 2007, **26**, 702–712.

19 R. Tanaka, M. Yamashita and K. Nozaki, *J. Am. Chem. Soc.*, 2009, **131**, 14168–14169.

20 (*a*) S. Enthaler, K. Junge and M. Beller, *Angew. Chem., Int. Ed.*, 2008, **47**, 3317–3321; (*b*) S. Gaillard and J.-L. Renaud, *ChemSusChem*, 2008, **1**, 505–509; (*c*) A. Correa, O. G. Mancheño and C. Bolm, *Chem. Soc. Rev.*, 2008, **37**,

1108–1117; (*d*) C. Federsel, A. Boddien, R. Jackstell, R. Jennerjahn, P. J. Dyson, R. Scopelliti, G. Laurenczy and M. Beller, *Angew. Chem., Int. Ed.*, 2010, **49**, 1–6; (*e*) R. Langer, Y. Diskin-Posner, G. Leitus, L. J. W. Shimon, Y. Ben-David and D. Milstein, *Angew. Chem., Int. Ed.*, 2011, **50**, 9948–9952.

21 R. M. Bullock, *Chem. – Eur. J.*, 2004, **10**, 2366–2374.

22 (*a*) S. Chakraborty, O. Blacque, T. Fox and H. Berke, *ACS Catal.*, 2013, **3**, 2208–2217; (*b*) E. Peterson, A. Y. Khalimon, R. Simionescu, L. G. Kuzmina, J. A. K. Howard and G. I. Nikonov, *J. Am. Chem. Soc.*, 2009, **131**, 908; (*c*) V. K. Dioumaev and R. M. Bullock, *Nature*, 2000, **424**, 530–532.

23 (*a*) S. Chakraborty, O. Blacque, T. Fox and H. Berke, *Chem. – Asian J.*, 2014, **9**, 328–337; (*b*) A. Dybov, O. Blacque and H. Berke, *Eur. J. Inorg. Chem.*, 2011, 652–659; (*c*) S. Chakraborty, O. Blacque, T. Fox and H. Berke, *Chem. – Asian J.*, 2014, **9**, 2896–2907.

24 S. Chakraborty, O. Blacque, T. Fox and H. Berke, *Chem. – Eur. J.*, 2014, **20**, 12641–12654.

25 S. Chakraborty and H. Berke, *ACS Catal.*, 2014, **4**, 2191–2194.

26 (*a*) P. J. Walsh, F. J. Hollander and R. G. Bergman, *J. Am. Chem. Soc.*, 1988, **110**, 8729–8731; (*b*) P. J. Walsh, F. J. Hollander and R. G. Bergman, *Organometallics*, 1993, **12**, 3105–3123; (*c*) J. L. Bennett and P. T. Wolczanski, *J. Am. Chem. Soc.*, 1994, **116**, 2179–2180; (*d*) J. de With and A. D. Horton, *Organometallics*, 1993, **12**, 1493–1496.

27 M. W. Bouwkamp, A. A. Batinas, P. T. Witte, T. Hubregtse, J. Dam, A. Meetsma, J. H. Teuben and B. Hessen, *Organometallics*, 2008, **27**, 4071–4082.

28 (*a*) Z. Chen, H. W. Schmalle, T. Fox and H. Berke, *Dalton Trans.*, 2005, 580–587; (*b*) J. Höck, H. Jacobsen, H. W. Schmalle, G. R. J. Artus, T. Fox, J. I. Amor, F. Bäth and H. Berke, *Organometallics*, 2001, **20**, 1533–1544; (*c*) F. Furno, T. Fox, H. W. Schmalle and H. Berke, *Organometallics*, 2000, **19**, 3620–3630; (*d*) F. Liang, H. Jacobsen, H. W. Schmalle, T. Fox and H. Berke, *Organometallics*, 2000, **19**, 1950–1962; (*e*) Y. Zhao, H. W. Schmalle, T. Fox, O. Blacque and H. Berke, *Dalton Trans.*, 2006, 73–85.

29 L. Bencze and J. Kohan, *Inorg. Chim. Acta*, 1982, **65**, L17–L19.

30 A. A. Danopoulos, A. R. Wills and P. G. Edwards, *Polyhedron*, 1990, **9**, 2413–2418.

31 CCDC 888516 (for **4b(*trans*)**) and 888517 (for **6b(*cis*)**), 960495 (for **2a(*anti*)**) 960496 for **2b(*syn*)**) contain the supplementary crystallographic data (excluding structure factors) for this paper.

32 (*a*) *Agilent Technologies (formerly Oxford Diffraction)*, Yarnton, England, 2011; (*b*) R. C. Clark and J. S. Reid, *Acta Crystallogr., Sect. A: Fundam. Crystallogr.*, 1995, **51**, 887–897; (*c*) G. M. Sheldrick, *Acta Crystallogr., Sect. A: Fundam. Crystallogr.*, 2008, **64**, 112–122; (*d*) L. J. Farrugia, *J. Appl. Crystallogr.*, 1999, **32**, 837; (*e*) A. L. Spek, *J. Appl. Crystallogr.*, 2003, **36**, 7–13; (*f*) K. Brandenburg, *DIAMOND*, Crystal Impact GbR, Bonn, Germany, 2007.